PREDICTION OF WARM SEASON CONVECTIVE SYSTEMS
USING A MATRIX OF 19 WRF PHYSICAL CONFIGURATIONS

William A. Gallus, Jr. and Isidora Jankov
Iowa State University, Ames, Iowa

1. INTRODUCTION

A matrix of 19 WRF members was created using different combinations of physical schemes and run for eight IHOP (International H_2O Project) convective cases. Cases were purposely selected to have significant rainfall observed and/or forecasted in the IHOP domain over the central United States. For each case, three different treatments of convection were used: the Kain-Fritsch (KF) scheme (Kain and Fritsch 1992), the Betts-Miller-Janjic (BMJ) scheme (Betts 1986, Betts and Miller, 1986, Janjic 1994), and the use of no convective parameterization. For each of these three choices, three different microphysical schemes were used, Lin et al. (1983), NCEP-5 class, and Ferrier (Ferrier et al., 2002). Within these nine configurations, two different planetary boundary layer schemes were used, MRF (Troen and Mahrt, 1986) and Eta (Janjic 1994). This 18-member matrix was supplemented with one additional member using the thermal diffusion surface physics scheme instead of the OSU scheme used for the full 18-member matrix. The 'control' used the configuration run at NOAA's FSL in real time during IHOP, and it used the KF convective scheme, MRF PBL scheme and NCEP class-5 microphysics.

2. RESULTS

Subjective analysis of rainfall forecasts indicated that the greatest variability in the forecasts came from changes in the choice of convective scheme, although noticeable impacts also occurred from changes in the microphysics or PBL scheme. The Eta PBL scheme seemed to be moister and slightly cooler than the MRF scheme, which impacted convective system development. The Lin et al. microphysics typically resulted in the most rainfall, and the NCEP-5 class scheme produced the least. The surface physics scheme generally had less noticeable impacts on the forecast.

Equitable Threat Scores (ETS) for all model versions for the first six hours of each 24 hour forecast (Table 1) indicate relatively well-predicted light precipitation with almost no skill for heavier thresholds. Three out of eight cases exhibited relatively high predictability for all thresholds, and two cases exhibited very low predictability.

Corresponding author address: William A. Gallus, Jr., ISU, 3025 Agronomy Hall, Ames, IA. Email: wgallus@iastate.edu.

Threshold (in.)	.01	.25	.50	1.0
June 19, 12Z	**.353**	**.212**	**.150**	**.068**
June 13, 00Z	.251	**.275**	**.236**	**.157**
June 15, 06Z	*.090*	*.023*	*.004*	*.000*
June 04, 00Z	**.332**	**.210**	**.134**	**.078**
May 23, 12Z	.176	*.026*	*.000*	*.000*
May 24, 18Z	.209	.074	.039	*.003*
June 02, 12Z	**.407**	.145	*.000*	*.000*
May 16, 06Z	**.355**	*.024*	*-.003*	*.000*

Table 1. ETS values for all cases for the 00-06 h forecast period, with relatively good forecasts in boldface and relatively bad forecasts italicized.

ETSs for the 12-18 hour forecast period show less skill, as might be expected, with once again higher scores for lighter amounts (Table 2). Note that a good (bad) forecast at earlier times is not necessarily followed by a good (bad) forecast at later times. The ETS for .01 inch rainfall for the 2 June case was .407 in the 00-06 h period but fell to .007 by 12-18 h. The 15 June case is one where ETSs were much higher at later times than at earlier times.

Threshold (in.)	.01	.25	.50	1.0
June19, 12Z	.171	.171	.147	.074
June 13, 00Z	.188	.068	.031	*.000*
June 15, 06Z	.184	.274	.259	.060
June 04, 00Z	.203	.143	**.152**	**.056**
May 23, 12Z	**.328**	.105	*-.001*	*-.002*
May 24, 18Z	**.273**	.151	.040	*.000*
June 02, 12Z	*.007*	*-.002*	*-.001*	*.000*
May 16, 06Z	*.028*	*.009*	*-.001*	*.000*

Table 2. As in Table 1 except for the 12-18 h forecast period.

Bias analyses (not shown) indicate that for light amounts, both convective schemes have substantially high biases during the early hours of the forecast. The worst overestimate occurs in the 06-12 h period. For heavier thresholds, bias trends are not as pronounced.

In addition, analyses of ETS and bias indicate that there is no model configuration that stands out as best. The best configuration varies both with time and threshold. For example, for the first six-hour period (00-06 h), the non-convective run with the ETA PBL and Lin et al. microphysics earns the highest ETSs for amounts lower than 0.5 inches, while for the heavier thresholds, the run with the KF

scheme, ETA PBL and Ferrier microphysics (MP5) has the highest ETS (Table 3). Later, during the 06-12 h period there is no clear winner (not shown). For the 12-18 h period the non-convective run with the MRF PBL and Lin microphysics has the highest skill for amounts lower than .5 inches (Table 4), but in the 18-24 h period the KF run with the MRF PBL and Lin et al. microphysics has the best score for amounts lower than 1 inch (not shown). In summary, over the four time periods, and for six different rainfall thresholds, the best ETSs by schemes are: Lin (11), NCEP5 (7), Ferrier (5), ETA PBL (13), MRF PBL (10), KF scheme (12), NC (8), and BMJ (4). It should be noted that differences in ETSs are usually small.

In order to test the sensitivity to physics changes, spread ratios (SRs) when two of three model physic schemes are held fixed and the third varied (i.e PBL scheme and CP scheme are constant while microphysics varies) were computed for two thresholds using pairs of runs (Table 5).

Threshold (in.)	.01	.10	.50	1.0
BMJETAMP2	.246	.167	.100	.053
BMJETAMP4	.249	.182	.070	.026
BMJETAMP5	.249	.177	.079	.029
BMJMRFMP2	.249	.179	.099	.054
BMJMRFMP4	.249	.178	.100	.046
BMJMRFMP5	.252	.180	.074	.038
KFETAMP2	.235	.187	.077	.055
KFETAMP4	.242	.201	.066	.033
KFETAMP5	.272	.205	.090	**.063**
KFMRFMP2	.255	.196	.073	.059
KFMRFMP4	.265	.211	.067	.041
KFMRFMP5	.276	.206	.075	.038
NCETAMP2	**.349**	**.247**	.086	.044
NCETAMP4	.327	.215	.048	.022
NCETAMP5	.298	.203	.055	.041
NCMRFMP2	.308	.201	.066	.039
NCMRFMP4	.304	.191	.057	.029
NCMRFMP5	.311	.208	.057	.032

Table 3. Average ETSs for all cases and different physics combinations for the 00-06 forecast period and different precipitation thresholds. MP2 represents Lin et al. scheme, MP4 NCEP-5 class, and MP5 Ferrier microphysics. Boldface indicates best single value.

The greatest spread (Table 5) occurs in runs using different convective schemes at both thresholds. Spread is especially large for the heavier threshold after 6 hours and becomes large even for changes to the PBL and microphysical schemes. For lighter precipitation thresholds, sensitivities to the PBL and microphysics scheme are comparable, while for the heavier thresholds, sensitivity to the PBL scheme is occasionally noticeably higher than to microphysics.

Threshold (in.)	.01	.10	.50	1.0
BMJETAMP2	.167	.141	.064	.020
BMJETAMP4	.162	.148	.065	.014
BMJETAMP5	.160	.145	.053	.020
BMJMRFMP2	.176	.148	.065	.022
BMJMRFMP4	.168	.145	.043	.009
BMJMRFMP5	.160	.126	.061	.015
KFETAMP2	.160	.145	.102	.029
KFETAMP4	.168	.157	.089	.018
KFETAMP5	.133	.122	.105	.027
KFMRFMP2	.177	.146	.103	.047
KFMRFMP4	.169	.155	.091	.027
KFMRFMP5	.172	.141	.085	.023
NCETAMP2	.156	.152	.079	.016
NCETAMP4	.156	.152	.079	.016
NCETAMP5	.164	.151	.057	.014
NCMRFMP2	**.239**	**.213**	.113	.043
NCMRFMP4	.211	.195	.118	.040
NCMRFMP5	.181	.159	.077	.034

Table 4. As in Table 3 except for 12-18h period.

		Forecast Period			
Threshold (in.)	**Physics**	00-06 h	06-12 h	12-18 h	18-24 h
0.01	**Micro.**	2.41	1.69	2.00	2.31
	PBL	1.58	2.02	2.55	3.23
	Conv.	11.7	4.16	3.79	5.21
0.5	**Micro.**	4.07	4.00	9.50	13.8
	PBL	3.20	9.89	10.72	18.7
	Conv.	6.61	48.0	25.00	52.3

Table 5. SR as a function of time for runs using different physics schemes at .01 and .5 in. precipitation thresholds.

		Forecast Period			
Threshold (in.)	**Physics**	**00-06 h**	**06-12 h**	**12-18 h**	**18-24 h**
0.01	**Micro.**	**0.66**	**0.55**	**0.40**	**0.32**
	PBL	**0.67**	**0.48**	**0.29**	**0.21**
	Conv.	**0.36**	**0.22**	**0.17**	**0.10**
0.5	**Micro.**	**0.40**	**0.34**	**0.21**	**0.17**
	PBL	**0.39**	**0.29**	**0.14**	**0.09**
	Conv.	**0.22**	**0.10**	**0.07**	**0.03**

Table 6. As in Table 5, except for Squared Correlation Coefficient.

Squared correlation coefficient (r^2) values are lowest for both thresholds during the whole forecast period when the convective treatment is changed (Table 6). The r^2 when microphysics and

PBL scheme are varied are generally comparable but changes in microphysics seem to have slightly less impact on the forecast than changes in the PBL scheme, especially at later times. The largest differences between the impact of changes in convective treatment and changes in other schemes occur during the earliest forecast periods. Thus, to achieve a large spread of solutions within 6 or 12 h, it is important to vary the convective treatment.

A factor separation approach (Stein and Alpert 1993) also has been used to examine in more detail the impact of different model physics on precipitation forecasts as well as interactions among those different physics. The factor separation approach applied to system average rain rate supported the SR and r^2 results indicating that the choice of convective scheme impacted the forecast the most. Table 7 shows the impacts on

		Forecast period			
Threshold (in.)	Different model configurations	00-06	06-12	12-18	18-24
0.01	$(f_1 - f_0)/f_0$ (%)	52	55	37	10
	Area (pts.)	1270	1317	1143	964
	$(f_2 - f_0)/f_0$ (%)	5	16	16	39
	Area (pts.)	3367	3073	2907	2154
	$(f_3 - f_0)/f_0$ (%)	10	14	12	22
	Area (pts.)	2999	2899	2614	2095
	$\hat{f}_{12} / f_0$ (%)	12	24	8	73
	$\hat{f}_{13} / f_0$ (%)	-25	-24	-14	16
0.5	$(f_1 - f_0)/f_0$ (%)	3	45	21	11
	Area (pts.)	141	220	178	110
	$(f_2 - f_0)/f_0$ (%)	2	20	8	25
	Area (pts.)	250	336	369	315
	$(f_3 - f_0)/f_0$ (%)	-2	1	1	11
	Area (pts.)	222	358	311	296
	$\hat{f}_{12} / f_0$ (%)	8	-22	2	25
	$\hat{f}_{13} / f_0$ (%)	-24	-36	-16	-11

Table 7. Percentage changes in average rain rate due to changes in physics from control run (f_0) where f_1 represents run where no convective scheme is used and f_2, and f_3 represent runs where microphysical scheme has been changed from MP4 to MP2 and MP5, respectively. Area coverage of rain also shown along with synergistic terms (f_{12} and f_{13} with hats) due to interactions of physical schemes.

system rain rate of changes from the KF scheme to no convective scheme and from MP4 to MP2 and MP5 microphysics for 2 thresholds. The change in convective scheme greatly increased rain rates when the .01 inch threshold was examined. Both microphysical changes also increased rain rate, although to a lesser extent. The control rain region covered 2638, 2683, 2291 and 1750 points during the 0-6, 6-12, 12-18 and 18-24 h periods, respectively. It can be seen that the switch to no convective scheme greatly reduced the areal coverage of precipitation, while the change to both MP2 and MP5 microphysics increased areal coverage. Results differed slightly for the heavier threshold (control rain coverage was 159, 235, 202, and 163 points at the 4 times).

When the approach was applied to total domain rain volume (Table 8), the choice of microphysics (f_2, f_3) had the biggest impact on total water volume. The microphysics schemes seem to affect the areal coverage of heavy rain and the peak amounts. Total areal coverage changes in such a way that system average rain rate may not change much but total rain volume in the domain does. Very large changes are especially noticeable for the .5 inch amount. The synergistic term in the factor separation analysis, providing information on how changes in two physical schemes within a run interacted to change the rainfall, varied greatly as different combinations of physics were used (not shown). The complex behavior complicates interpretation of the scheme

		Forecast Period			
Threshold (in.)	Different model configurations	00-06	06-12	12-18	18-24
0.01	Obs. volume x10^{12} (kg)	1.58	2.26	2.26	2.77
	CTL volume x10^{12} (kg)	1.52	1.97	1.64	1.28
	$(f_1 - f_0)/f_0$ (%)	16	15	14	20
	$(f_2 - f_0)/f_0$ (%)	37	32	53	94
	$(f_3 - f_0)/f_0$ (%)	26	22	22	46
	$\hat{f}_{12} / f_0$ (%)	-5	-9	-1	-69
	$\hat{f}_{13} / f_0$ (%)	11	-7	-1	-3
0.5	Obs. volume x10^{12} (kg)	0.77	1.16	1.28	1.67
	CTL volume x10^{12} (kg)	0.51	0.74	0.59	0.18
	$(f_1 - f_0)/f_0$ (%)	7	25	-4	16
	$(f_2 - f_0)/f_0$ (%)	59	72	94	180
	$(f_3 - f_0)/f_0$ (%)	37	54	41	101
	$\hat{f}_{12} / f_0$ (%)	0.0	-25	-20	-83
	$\hat{f}_{13} / f_0$ (%)	14	-15	-39	-27

Table 8: As in Table 7, except for domain average rain volume, with areal coverage no longer shown. Observed and control run rain volume are included.

interactions.

Finally, because no single member of the 19-member matrix consistently works better than the others, the matrix (18 members using the OSU surface schemes) was evaluated as an ensemble forecasting system. Areas under discrete ROC (relative operating characteristic) curves (calculated using the trapezoidal method) at different thresholds (Fig. 1) indicate relatively skillful forecasts but primarily for lighter amounts and earlier forecast times. These skill measures are comparable to those found in Eta ensembles using mixed convective schemes and mesoscale initialization adjustments.

3. SUMMARY

A matrix of 19 WRF members was created using different physical scheme combinations and run for eight IHOP cases. For the matrix, three different convective treatments (BMJ, KF and no convective scheme), two different PBL schemes (MRF and ETA) and three different sets of microphysics (NCEP-5, Lin et al., and Ferrier), were used, with one additional member using the thermal diffusion surface physics instead of the OSU scheme.

In order to test the sensitivity to physics changes, SRs, correlation coefficients and factor separation terms were calculated when two of three model physics were held fixed. The highest sensitivity was found to be to the choice of convective treatment, in good agreement with subjective impressions based on precipitation plots. The sensitivity to the PBL and microphysical schemes is much less and comparable for lighter precipitation while for heavier thresholds sensitivity to microphysics is higher. The factor separation analysis suggests the convective scheme greatly affects system rain rates but the microphysical scheme may have the greatest affect on domain rain volume. Finally, because this research shows that there is no particular combination of WRF model physics schemes that dominates in skill over time for these warm season convective events, this matrix of WRF model runs may form a good ensemble if the ensemble spread is sufficiently large. The use of this mixed physics ensemble will be investigated in more detail in the future.

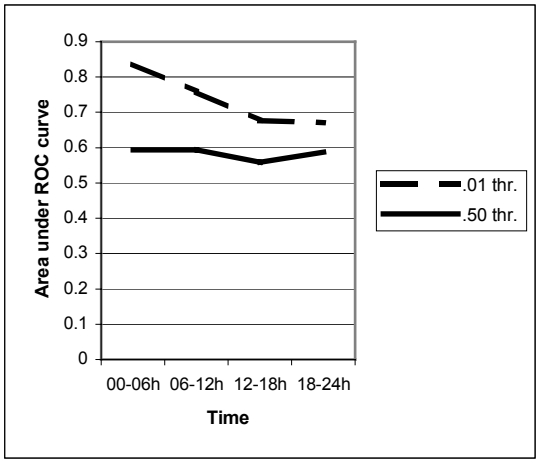

Figure 1. Areas under ROC curves for an ensemble consisting of 18 different physics runs at .01 and .5 inch thresholds for four 6h forecast periods.

4. ACKNOWLEDGEMENTS

This research was funded in part by NSF Grant 0226059 and by a NOAA grant administered through the Forecast Systems Laboratory.

5. REFERENCES

Betts, A. K., 1986: A new convective adjustment scheme. Part I: Observational and theoretical basis. *Quart. J.Roy. Meteor. Soc*., **112**, 677-692.

Betts, A. K., and M. J. Miller, 1986: A new convective adjustment scheme. Part II: Single column test using GATE wave, BOMEX, and arctic air-mass data sets. *Quart. J. Roy. Meteor. Soc.*, **112**, 693-709.

Ferrier, B. S., Y. Jin, T. Black, E. Rogers, and G. DiMego, 2002: Implementation of a new grid-scale cloud and precipitation scheme in NCEP Eta model. *Preprints, 15th Conf. On Numerical Weather Prediction,* San Antonio, TX, Amer. Meteor. Soc., 280-283.

Janjic, Z. I., 1994: The step-mountain Eta coordinate model: Further developments of the convection closure schemes. *Mon. Wea. Rev*., **122**, 927-945.

Kain, J. S., and J. M. Fritsch, 1992: The role of convective “trigger function” in numerical forecasts of mesoscale convective systems. *Meteor. Atmos. Phys.*, **49**, 93-106.

Lin, Y.-L., R. D. Farley, and H. D. Orville, 1983: Bulk parameterization of the snow field in a cloud model. *J. Climate Appl. Meteor.,* **22**, 1065-1092.

Stein, U. and P. Alpert, 1993: Factor separation in numerical simulations. *J. Atmos. Sci.*, **50**, 2107-2115.

Troen, I. and Mahrt, L., 1986: A simple model of the atmospheric boundary layer: Sensitivity to surface evaporation. *Boundary-Layer Meteor*. **47**, 129-148.